Supplemental Figures
with
Figure legends

January 2022

An active zone state switch concentrates and immobilizes voltage gated Ca^{2+} channels to promote long-term plasticity

Tina Ghelani[1-3], Marc Escher[1], Ulrich Thomas[4], Klara Esch[1], Janine Lützkendorf[1], Harald Depner[1], Marta Maglione[1], Pierre Parutto[6-7], Scott Gratz[9], Stefanie Ryglewski[5], Alexander Walter[2], David Holcman[6,8], Kate O'Connor Giles[9-10], Martin Heine[5]* and Stephan Sigrist [1,3]*

*: Correspondence

[1]Institute for Biology and Genetics, Freie Universität Berlin, Takustraße 6, 14195 Berlin, Germany.
[2]Molecular and Theoretical Neuroscience Leibniz-Forschungs institut für Molekulare Pharmakologie (FMP) im CharitéCrossOver (CCO) Charité - University Medicine Berlin Charité Campus Mitte Charité Platz 110117 Berlin
[3]Institute for Biology and Genetics, Freie Universität Berlin, Takustraße 6, 14195 Berlin, Germany; NeuroCure Cluster of Excellence, Charité Universitätsmedizin, Charitéplatz 1, 10117 Berlin,
[4]Research Group Molecular Physiology, Leibniz-Institute for Neurobiology, Brenneckestr. 6, 39118 Magdeburg, Germany
[5]Institute of Developmental Biology and Neurobiology, Johannes Gutenberg University Mainz, Mainz, Germany
[6]Group of Applied Mathematics and Computational Biology, IBENS, Ecole Normale Superieure, Paris, France
[7]Dementia Research Institute at University of Cambridge, Department of Clinical Neurosciences, Cambridge CB2 0AH, United Kingdom
[8]Churchill College, University of Cambridge, Cambridge CB3 0DS, UK
[9]Department of Neuroscience, Brown University, Providence, Rhode Island 02912
[10]Carney Institute for Brain Science, Brown University, Providence, RI 02912

Live in vivo localization microscopy (sptPALM) of CacmEOS4b molecules

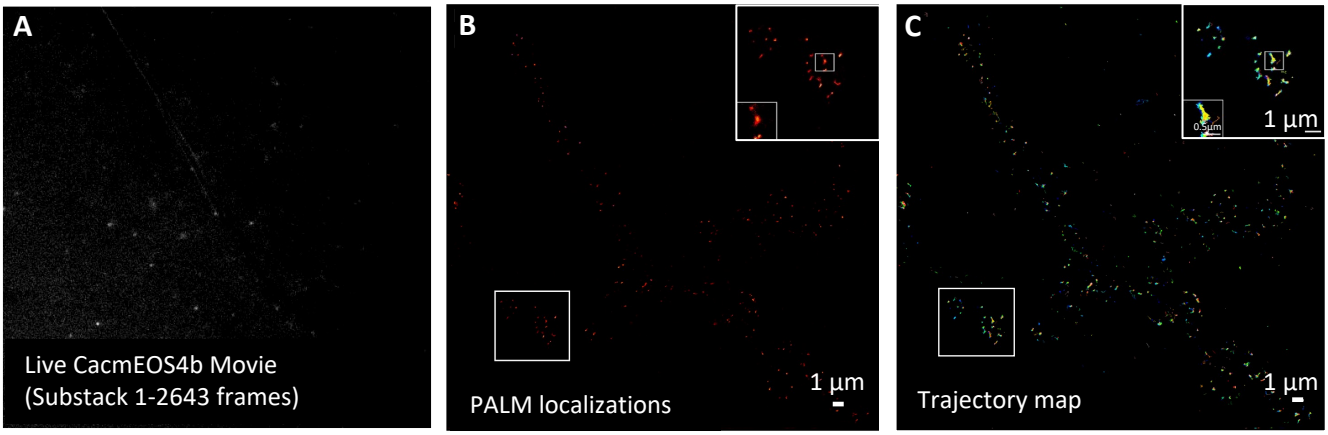

Localization accuracy and photon counts of CacmEOS4b molecules

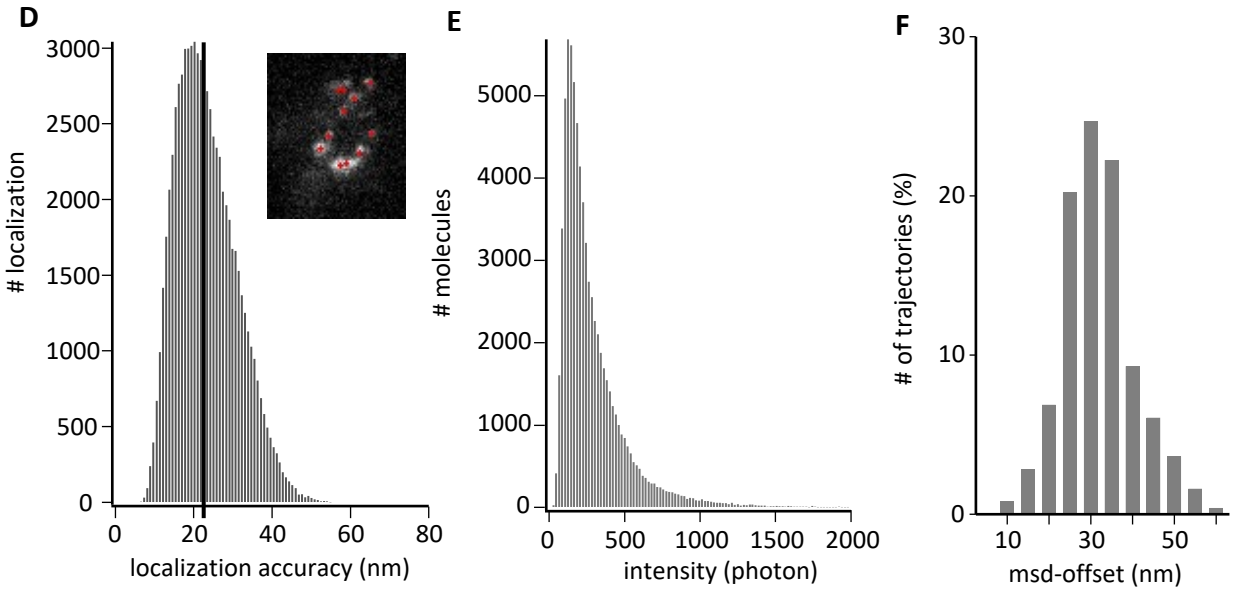

Supplemental Figure 1. Parameters of single molecule localization microscopy experiments in *Drosophila* larvae.
A-C) Representative movie of an entire *Drosophila* Muscle 6 NMJ imaged live, *in vivo* with sptPALM for 5000 frames at 20 Hz frame rate (1-2643 frames shown) (A), the PALM localization map (B) and trajectory map (C) derived from analysis of this movie. Scale Bars B-C= 1 µm and inset C 0.5 µm. D) Localization accuracy of individual events (n=72713) within 6 presynaptic boutons from 6 animals recorded for 2500-5000 frames. The mean localization accuracy is 23.7 ± 7.7 nm (median 22.7 nm IQR 17.8 nm / 28.7 nm). Insert show single frame image of a bouton and the detected molecule localization (red crosses). E) Intensity distribution of detected molecules, mean photon count for individual mEOS4b tagged channels was 297.3 ± 227.9 photons (median 227.3 IQR 152.7 / 364.1) from same experiments as in E. F) Trajectories from immobile/confined molecules that resulted in a MSD-curves parallel to the x-axis of the MSD versus time blot (Fig.1O) were taken as independent control for the localization accuracy within sptPALM experiments after reconstruction of individual trajectories, here only trajectories longer than 10 points were included. The average offset of the immobilized MSD blot was 31.3 nm IQR 25.9 / 36.6 nm. The viability of *Drosophila* larvae filet preparation within the imaging experiment was tested by prolonged imaging of individual NMJs. The frequency of spontaneous activity was monitored by calcium imaging of postsynaptic events in animals expressing the calcium sensor Syn-GCamp6f within the muscular membrane and the CacmEOS4b within the presynaptic bouton.

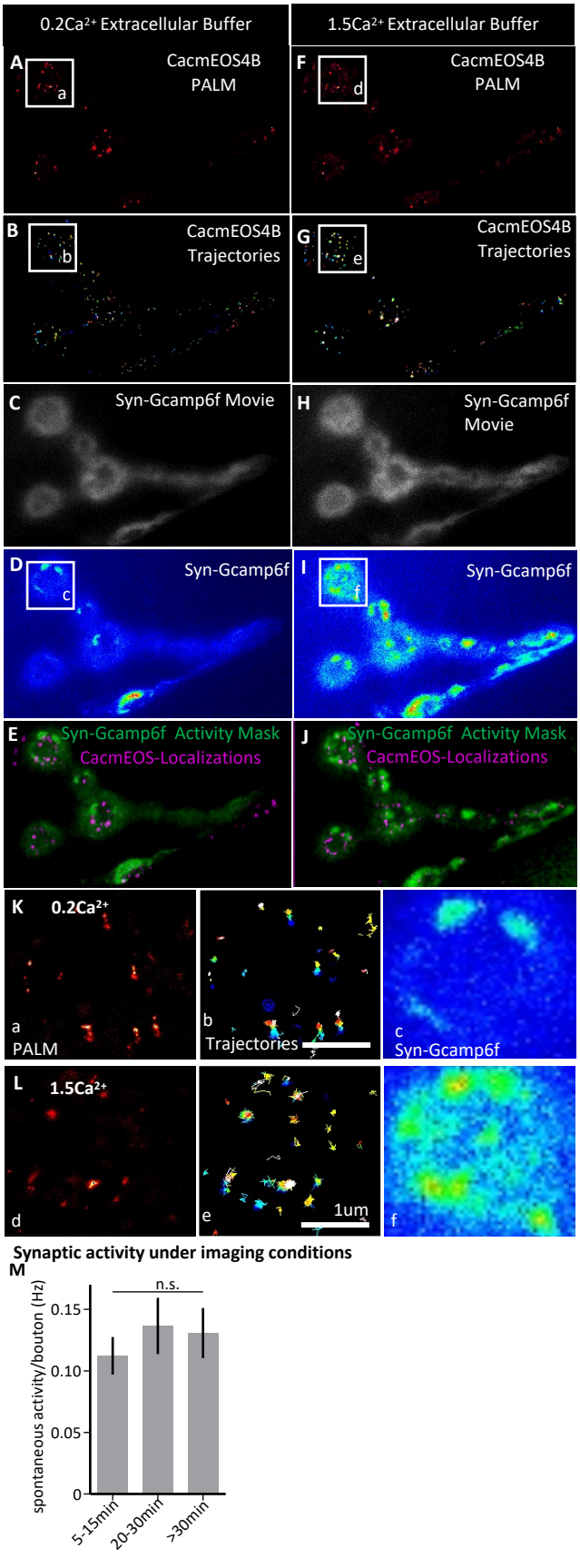

Supplemental Figure 2. Parameters of single molecule localization microscopy experiments in *Drosophila* larvae. A-J) live imaging of third-instar larvae at muscle 4 of CacmEOS4b;;Syn-GCAMP6f was first imaged in low (0.2mM Ca^{2+}) (**A-E**) and then in control (1.5mM Ca^{2+}) (**F-J**) extracellular imaging solution. Here a live Syn-GCAMP6f recording was performed for 5000 frames at 50 Hz (C-E and H-J) and then sptPALM recording of CacmEOS4b was performed at 20 Hz for 5000 frames in (A-B and F-G). Accumulated activity masks of C or H are shown in D and E, or J and I, respectively. sptPALM image processing was applied to retrieve the PALM localizations and trajectories of Cac channels in **A, B, F** and **G.** Zoomed insets **a-f** are represented in **K** and **L. M** The vitality of larval body wall preparations in sptPALM experiments was evaluated by monitoring spontaneous activity in 1.5mM Ca^{2+} by postsynaptic Syn-GCamp6f. Repetitive recordings from individual NMJs over time resulted in a decay of spontaneous activity within 30 min. Imaging of different NMJ from different muscles did not result in a decay of spontaneous activity (M). Spontaneous activity measurements per bouton in 1.5mM Ca^{2+} extracellular imaging solution, no significant change in spontaneous activity was found over 30 min of recordings. Data are from 4 animals per condition from which 19 boutons for alternated illumination were analyzed. Differences were tested by one way ANOVA followed by a Newman-Keuls multiple comparison test. Statistical significance is denoted as asterisks ***$p < 0.001$. Scale Bar K-L=1 µm.

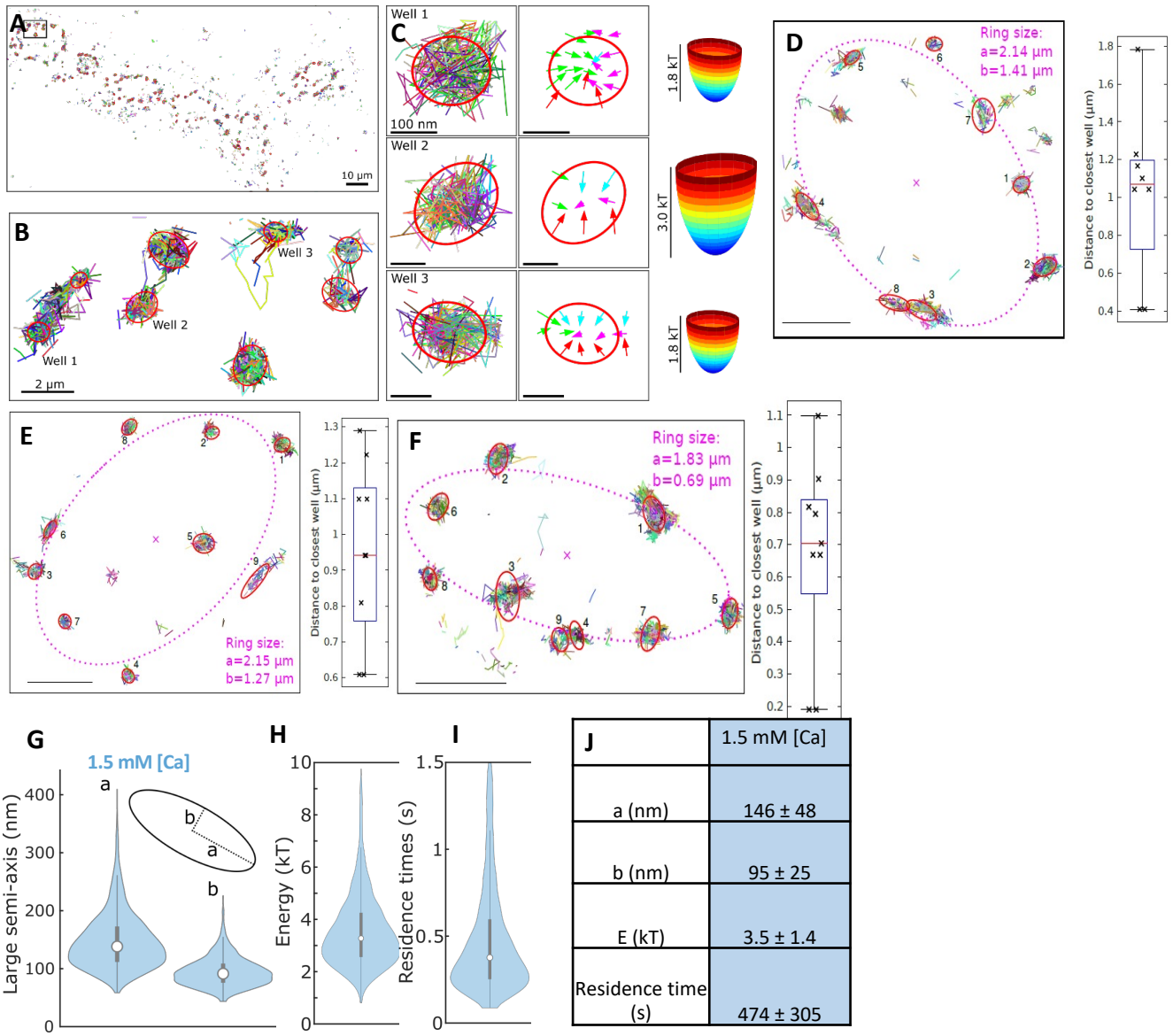

J	1.5 mM [Ca]
a (nm)	146 ± 48
b (nm)	95 ± 25
E (kT)	3.5 ± 1.4
Residence time (s)	474 ± 305

Supplemental Figure 3. In well analysis of live in vivo mobility of individual voltage Ca^{2+} channels at *Drosophila* NMJ synapses. A Single-particle trajectories of a representative NMJ displaying live Cac channel dynamics in third-instar CacmEOS4B larvae localized at AZs. **B** Blow-up of the region shown in (**A**) and possessing multiple wells. **C** Three examples of wells showing retained trajectories (left), their corresponding drift fields (middle) and energy representations (right). **D-F** Three regions showing wells organised in rings. **G-I** Cac well analysis of well semi-axes lengths; (**a** 146 ± 48nm, **b** 95 ± 25nm) (**G**), within well energy (**H**), and within well Cac channel residence time (**I**). **J** a detailed list of averages of within well characteristics N=50 images from 15 animals from which 2041 wells analysed. Single Particle Trajectory maps of Individual *Drosophila* NMJ boutons presenting endogenous Cacmeos4b wells imaged under control extracellular 1.5mM Ca^{2+} conditions display an inter-well distance of about 0.8µm.

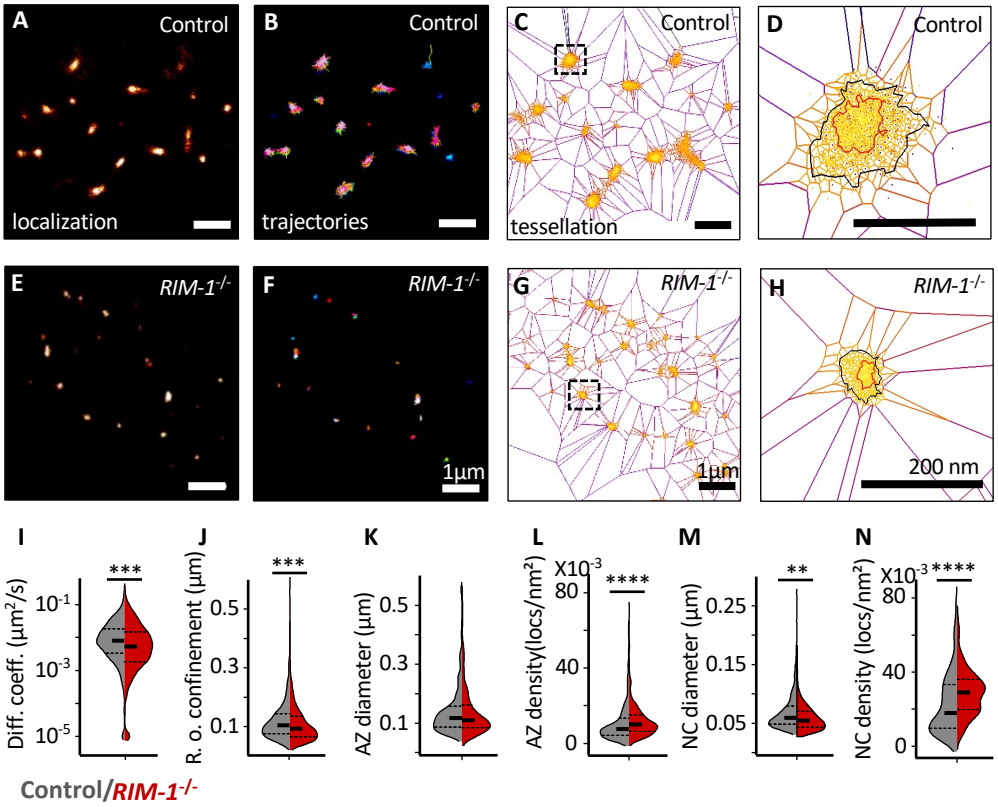

Suppl. Figure 4. Cac channels in *RIM-1* mutant AZs channel visualized for their live mobility and distribution at AZs. Live sptPALM imaging of CacmEOS4B (Control a.k.a Con) and *CacmEOS4B;;RIM-1*$^{-/-}$ mutants imaged in 1.5mM Ca^{2+} extracellular imaging buffer. Representative boutons displaying PALM images(A,E), trajectory maps (B-F) and representation of tessellation analysis (C-D,G-H) of individual Cac channels in a bouton of CacmEOS4B (control) and *CacmEOS4B;;RIM-1*$^{-/-}$ animals. Scale bar: A-C,E-G- 1µm; D,H:200nm. I-J, live sptPALM Diffusion coefficient and radius of confinement quantification of CacmEOS4B and *CacmEOS4B;;RIM-1*$^{-/-}$ NMJs, N=31 (Con) and 24 (*RIM-1-/-*) images from which 2192 (Con) and 1644 (*RIM*-1$^{-/-}$) confinement values. K-N; Tessellation analysis of the diameter and density of Cac channels localizations within Nanocluster (NC) (M-N) and Active Zone (AZ) (K-L) boundaries, N=31(Con) or 24 (*RIM-/-*) images from which 371 (Con) and 505 (*RIM-1-/-*) AZs analyzed. n=3 individual *RIM-1*$^{-/-}$ experiments were conducted with concurrent controls. PALM Data distribution is statistically tested with Kolmogorov-Smirnov test. Statistical significance is denoted as asterisks: *p < 0.05; **p < 0.01; ***p < 0.001; ****p < 0.0001.

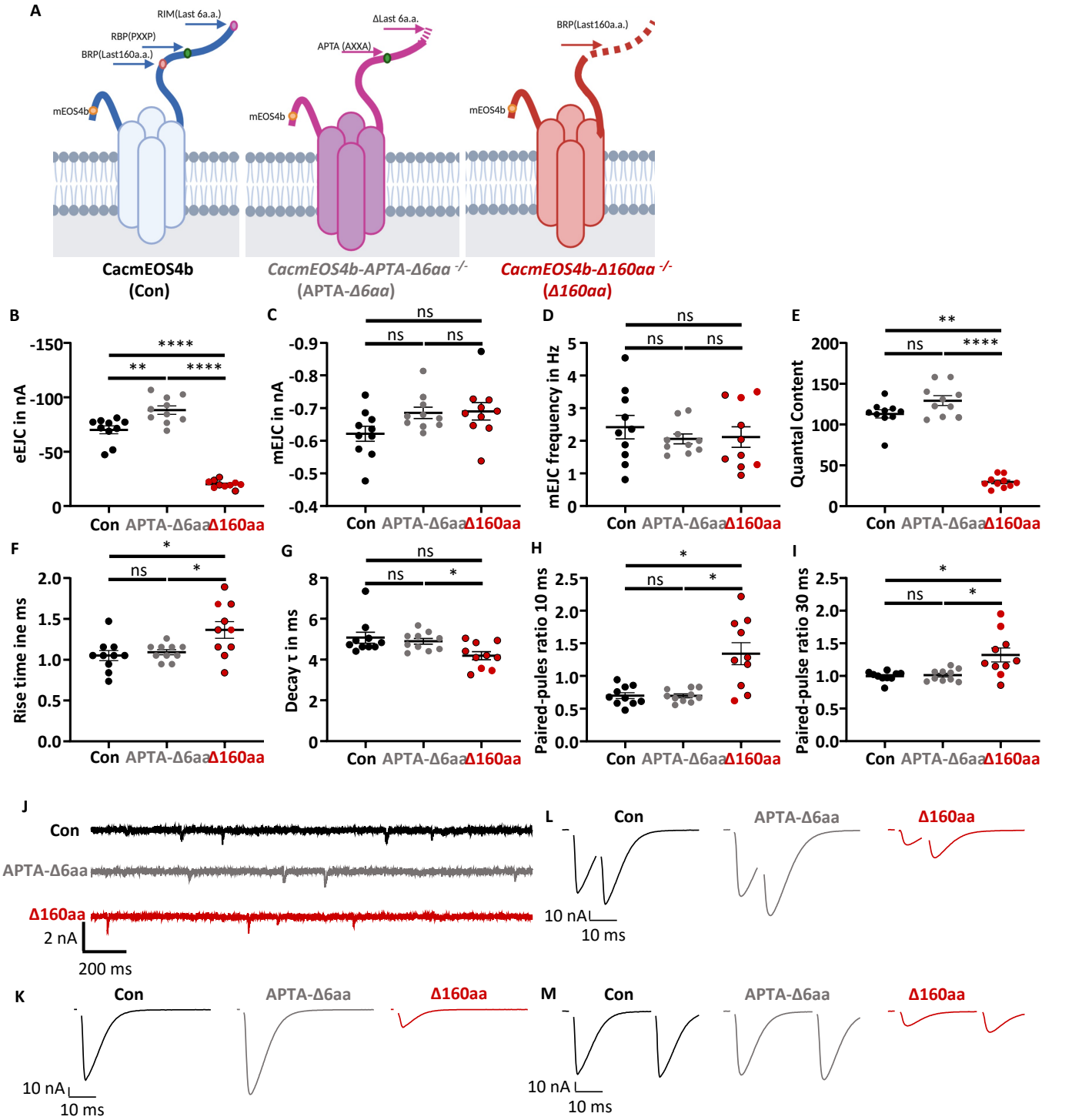

Suppl. Figure 5. Electrophysiological characterization of Cac channels in CacmEOS4B-APTA-Δ6aa and CacmEOS4BΔ160aa mutants. A: A Schematic diagram of on locus deletion mutants *CacmEOS4B-APTAΔ6aa* and *CacmEOS4B-Δ160aa* animals generated from endogenously tagged CacmEOS4B control flies. B-I: Electrophysiological recordings of CacmEOS4B, *CacmEOS4B-APTAΔ6aa* and *CacmEOS4BΔ160aa* animals using two-electrode voltage clamp (TEVC); quantifications for eEJC amplitude (B), mEJC amplitude (C) and mEJC frequency (D), Quantal content (E), eEJC rise time (F) and first order decay constant τ (G),and paired-pulse ratios (inter stimulus interval [ISI] of 10 ms (H) and 30 ms (I)). J-M: Representative traces of mEJC (J), eEJC (K), 10 ms ISI (L) and 30 ms ISI (M) TEVC recordings. Measurements were performed at third-instar larval muscle 6/7 NMJs of abdominal segments 2 and 3.

		pGADT7	
		BRP	**Control**
pGBKT7	Cacophony C-term	**+++++**	-----
	Δ304 aa	-----	-----
	Δ130 aa	**---++**	-----
	Δ81 aa	**---++**	-----
	Δ60 aa	**+++++**	-----
human laminin C (aa 66-230)		-----	

Supplemental Figure 6. Yeast two hybrid assay of testing interaction between various Cac Channels constructs of its C–terminal with a BRP N-terminal construct. **A)** range of Cac C-terminal deletion constructs namely: -d304aa, -d130aa, d81aa, -d60aa, d31aa were used as prey constructs. A strong interaction was observed with N-terminal BRP-D1 fragment (amino acid position 1—320) construct as the prey and Cac C-term full length construct, -d60aa and- d31aa baits. Interaction Legend: 5 clones were tested /double transformation; '-': no interaction ,'+': interaction. Positive control: pGADT7 SV40 large T-antigen (aa-84-708) vs. PGBKT7 Mouse p53 (aa72-390). Negative controls: PGBKT7 laminin and empty pGADT7 were used.

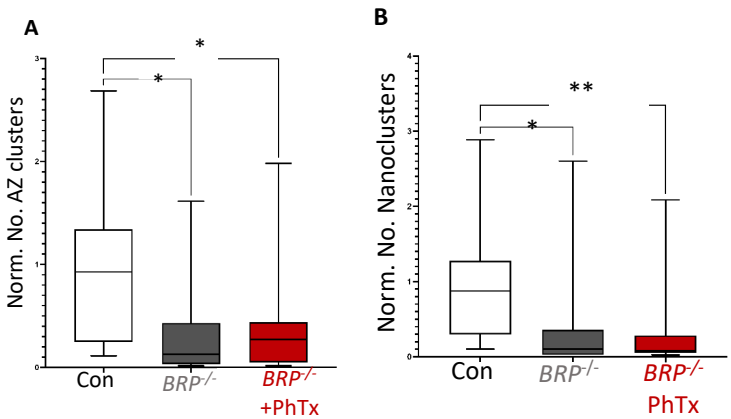

Supplemental Figure 7. Cac channels in BRP mutant AZs at normal or PhTx-treated remodeling AZs.
A-B, analysis from live sptPALM DATA depicting the number of Cac clusters identifiable with tessellation per image in CacmEOS4B (Con) and CacmEOS4B;*BRP*$^{-/-}$ (*BRP*$^{-/-}$) muscle 6/7 NMJs imaged and analyzed in Figure 5. N=30 images (CacmEOS4B or Con), N=8 images (*BRP*$^{-/-}$) and N=12 images (*BRP*$^{-/-}$) +PhTx) images. n=3 individual *BRP*$^{-/-}$ experiments conducted with concurrent controls.